Title

Tracing dissociation dynamics of CH3Br in the 3Q0 state with femtosecond extreme ultraviolet ionization

Authors

Vaida, Mihai E
Leone, Stephen R

Publication Date

2014-10-01

DOI

10.1016/j.chemphys.2014.01.015

Peer reviewed

Chemical Physics 442 (2014) 41–47

Contents lists available at ScienceDirect

Chemical Physics

journal homepage: www.elsevier.com/locate/chemphys

Tracing dissociation dynamics of CH_3Br in the $^3Q_0$ state with femtosecond extreme ultraviolet ionization

Mihai E. Vaida [a], Stephen R. Leone [a,b,c,*]

[a] Department of Chemistry, University of California, Berkeley, CA 94720, United States
[b] Department of Physics, University of California, Berkeley, CA 94720, United States
[c] Chemical Sciences Division, Lawrence Berkeley National Laboratory, Berkeley, CA 94720, United States

ARTICLE INFO

Article history:
Available online 11 February 2014

Keywords:
Femtosecond
High order harmonic generation
Photodissociation
Mass spectrometry

ABSTRACT

The ultrafast photodissociation dynamics of gas phase CH_3Br molecules in the red wing of the A-band, i.e. the first molecular adsorption continuum, is investigated by pump–probe spectroscopy. The experiment employs femtosecond laser pulses at 266 nm in the ultraviolet to dissociate the molecule and high order harmonic extreme ultraviolet pulses in conjunction with time-of-flight mass spectrometry to ionize and detect the fragments. A dissociation time of 116 ± 25 fs is obtained from the pump–probe risetime of the Br^+ ion signal, which originates from formation of either or both $Br(^2P_{3/2})$ or $Br^*(^2P_{1/2})$. The timescale is in a good agreement with the previously calculated A-band dissociation time of CH_3Br using the anisotropy parameter β deduced from angular photodissociation experiments. Based on classical molecular dynamics simulations and previous spectroscopic information, the most likely pathway is dissociation of the CH_3Br molecule via the $^3Q_0$ state of the A-band, which correlates with the formation of the spin–orbit excited bromine fragment.

1. Introduction

The formation of reactive species, i.e. radicals, is of fundamental importance in various branches of chemical sciences and engineering. Particularly, the fate of complex chemical transformations is drastically influenced by the formation timescale of free radical fragments. Therefore, it is of considerable interest to probe the chemical bond breaking timescale, especially the distance over which the molecular fragments are fully formed and the bond completely dissolved.

In this paper femtosecond (fs) extreme ultraviolet (XUV) pulses are used to trace when the Br atom (and the corresponding CH_3 radical) appears as a free species after the photoexcitation of the CH_3Br molecule in the red wing of the A-band. The experimental procedure employed here is able to distinguish between the fragments produced via A-band dissociation and dissociative photoionization.

The A-band of CH_3Br can be accessed in the 170–270 nm spectral range with an absorption maximum around 200 nm [1–4]. The photodissociation of the methyl bromide molecule via A-band excitation was investigated in the gas phase by means of time-of-flight mass spectrometry and velocity map imaging by excitation at several wavelengths: 193 nm and 222 nm [5], 205 nm [6], 215.9 nm [7], 213–235 nm [8], 218–245 nm [9], and 240–280 nm [10]. In principle, two dissociation channels can be accessed by means of A-band excitation: (i) the Br-channel giving rise to the formation of a methyl radical and a ground state $Br(^2P_{3/2})$, and (ii) the Br^*-channel giving rise to methyl and a bromine atom in the spin–orbit excited state $Br(^2P_{1/2})$. The $^1Q_1$ state that correlates with the formation of Br is the main contributor to the absorption cross section of the A-band. However, in the red wing of the A-band (240–280 nm) the $^3Q_0$ and $^3Q_1$ states have significant absorption (see Ref. [11] and references therein). The $^3Q_0$ state correlates with the formation of Br^* while the $^3Q_1$ state correlates with the formation of Br. Experimentally it has been observed that the majority of Br^* fragments are produced by direct absorption to the $^3Q_0$ state [6]. However, Br fragments can be produced directly via excitation of the $^1Q_1$ and $^3Q_1$ states and also by a surface crossing mechanism via $^3Q_0$ state excitation [6].

The direct time-resolved dissociation dynamics of the gas phase CH_3Br molecule via A-band excitation has not been investigated so far. It was considered that CH_3Br may photodissociate faster than CH_3I (about 70 fs for CH_3I [12,13]) via the respective A-band excitations, because the CH_3Br A-band absorption is slightly higher in energy and lies on an even steeper region of the excited state potential than the CH_3I A-band [6]. However, investigations

* Corresponding author at: Department of Chemistry, University of California, Berkeley, CA 94720, United States. Tel.: +1 510 643 5467; fax: +1 510 643 1367.
E-mail address: srl@berkeley.edu (S.R. Leone).

http://dx.doi.org/10.1016/j.chemphys.2014.01.015
0301-0104/

employing photofragment anisotropy measurements provide an estimate of the dissociation time through the rotational period. Those investigations estimated the dissociation time of the gas phase CH_3Br molecules to be between 111 fs and 120 fs for the Br^* dissociation channel and considerably longer, 188 fs for the Br dissociation channel [9,10]. The Br^* is formed in a shorter time than Br, because the CH_3 is born 'hotter', i.e. has higher vibrational energy, when it is formed together with the Br-channel. Although the CH_3Br A-band absorption is energetically higher and steeper than the CH_3I A-band, the CH_3Br should dissociate slower than CH_3I because a larger amount of the energy available for the dissociation is released into the CH_3 fragment as internal energy, making CH_3 vibrationally hotter when it is produced from CH_3Br than CH_3I photodissociation [14].

The only time-resolved experiment has been performed on CH_3Br molecules physisorbed on insulating ultrathin magnesia films [15,16]. The CH_3Br molecules adsorbed on the magnesia surface were found to dissociate in about 150 fs after a two-photon excitation at a central wavelength of 266 nm. However, the dissociation time of the CH_3Br molecule adsorbed on the surface is influenced by the molecular adsorption geometry and the changes in electronic states due to the interaction between the molecule and the surface [16–18] and the result does not necessarily reveal the dissociation time of the free molecule.

Here femtosecond pump–probe spectroscopy in conjunction with high-harmonic ionization, time-of-flight mass spectrometry is employed to quantitatively characterize the dissociation time of the CH_3Br molecule in the gas phase. After excitation at the central wavelength of 266 nm, the bromine fragments are detected via ionization by a single photon XUV high harmonic laser pulse. Various scenarios for the CH_3Br dissociation at 266 nm are discussed and compared with a classical molecular dynamics simulation.

2. Experimental

The experimental setup employed in the present investigation consists of three main parts: (i) a commercial amplified femtosecond laser system with a central wavelength of 800 nm, (ii) a pump–probe setup in conjunction with a monochromatic fs extreme ultraviolet high harmonic source and (iii) an investigation chamber equipped with an effusive molecular beam and a time-of-flight mass spectrometer (TOF-MS). Fig. 1 shows a schematic representation of the fs XUV source together with the investigation chamber.

The fs-laser light is produced by a Ti:Sapphire mode locked oscillator continuously pumped by a 5 W Spectra Physics Millennia Nd:YVO laser. Pulse amplification is carried out by a Nd:YLF laser pumped Ti:Sapphire amplifier to yield 90 fs pulses, with an energy of 2.2 mJ at a repetition rate of 1 kHz. The amplified near infrared laser beam (800 nm) is divided into two arms to produce the pump and the probe laser beams. One arm (30% of the total power) is used to generate the pump beam at 266 nm by frequency tripling of the fundamental wavelength in a homebuilt crystal-based third harmonic generator. The pump beam is focused by a 100 cm lens into the investigation chamber.

The second arm (70% of the total power) is used to generate the probe pulse consisting of fs XUV light, which is produced by means of high harmonic generation [19–22].For the high harmonic generation the 800 nm light is focused by a 40 cm lens into a 3 mm long Ar gas cell. The generated harmonics that co-propagate with the residual fundamental laser light are separated by means of a plane grating. Subsequently, the harmonics are focused into the investigation chamber by a cylindrical mirror and a toroidal mirror. A 2 mm slit positioned inside the investigation chamber allows a single harmonic to pass into the interaction region; all the other harmonics are blocked. The pressure in the gas cell as well as the 800 nm light intensity and focus position are tuned to maximize the flux of the 15th harmonic (0.15 nm spectral width), which is the only harmonic used. The pump beam, 266 nm, is reflected into the interaction region by an aluminum mirror mounted in the vacuum apparatus a few millimeters above the XUV beam (cf. insert in Fig. 1). The pump and the probe beams are overlapped in the interaction region at a 1.5° angle.

In the investigation chamber a skimmed effusive molecular beam crosses the laser beam at a right angle. The ions formed in the interaction region are analyzed by a 130 cm long Wiley–McLaren TOF-MS positioned with the longitudinal axis perpendicular to the plane formed by the laser beam and the molecular beam. The molecular beam intersects the laser beams and the longitudinal axis of the TOF-MS at the same point between the repeller electrode and the extraction electrode of the TOF-MS.

The zero time delay between the pump and the probe pulse as well as the instrumental time response function is measured in situ by time-resolved spectroscopy using ionization of He following excitation of the He($1s^2$-1s3p) transition. The 1s3p state in He atom has a lifetime of about 1.76 ns [23] and is resonantly excited with a pump pulse tuned to the 15th harmonic. Subsequently, a probe pulse at 266 nm, which is delayed with respect to the pump pulse, ionizes the excited He atoms and the ions are detected by the TOF-MS. The resonantly excited He(1s3p) state is an instantaneous transition that results in a step function response when the excited He atom is ionized by the probe pulse at variable time

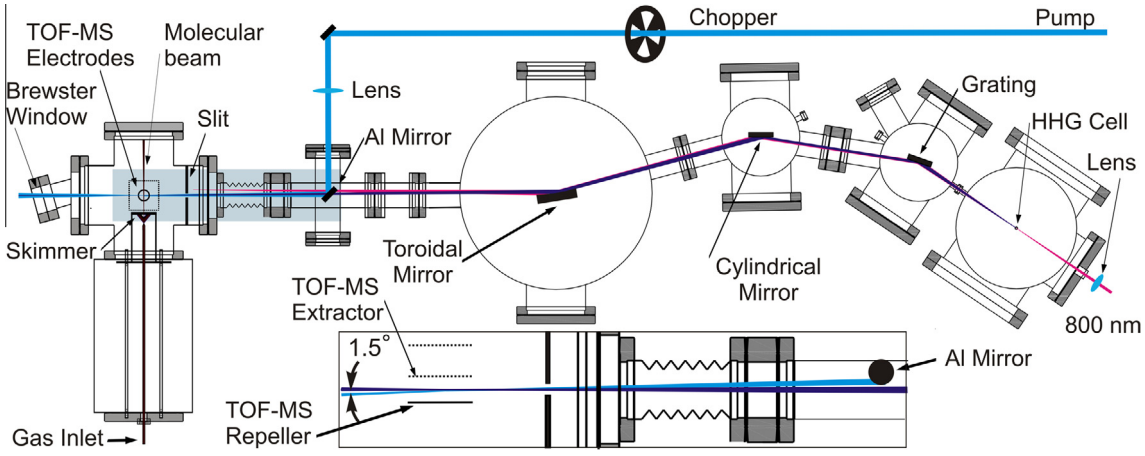

Fig. 1. Schematic layout of the fs-soft X-ray source together with the investigation chamber. Insert: detail illustrating the overlap between the pump and the probe beams into the interaction region.

delay. The instrumental response function is a convolution of the cross correlation function of the pump and probe pulses with a step function. Fig. 2 shows the instrumental time response function obtained by time-resolved spectroscopy of the He($1s^2$-1s3p) excitation, centered at the pump–probe zero time delay. The best fit to the measured data assuming that the laser pulses have a Gaussian shape gives a pulse cross correlation of 105 ± 10 fs.

For the photodissociation experiments presented below, CH_3Br (Sigma–Aldrich 99.5% purity) is used without further purification. All investigations are performed at room temperature.

3. Results

The experiments are designed to measure the dissociation time of the CH_3Br molecule excited at 266 nm and to gain insights into the possible dissociation pathways. The results provide an estimate of the timescale, through ionization of the Br atoms, when the atoms are far enough apart in the parent excited molecule, so that the electronic structure of the Br fragments is not influenced by the CH_3 radicals, and they can be considered free atoms. Fig. 3 shows a photoionization mass spectrum of CH_3Br recorded with the probe beam alone tuned to the 15th harmonic. The spectrum shows two intense peaks, one at 15 amu that corresponds to the CH_3^+ fragment and a double-peak structure at 94 and 96 amu that corresponds to the CH_3Br^+ parent molecule. A very low intensity double-peak structure is observed at 79 and 81 amu that corresponds to Br^+ ions. The mass spectrum in Fig. 3 reveals that the XUV probe beam alone is able to produce dissociative photoionization of the CH_3Br molecule. Interesting to note is the extremely low intensity of the Br^+ fragment with respect to the CH_3^+ fragment detected in the measured mass spectrum (cf. Fig. 3). The explanation of the fragment peak intensities is presented in the following section.

In order to investigate the photodissociation dynamics of the methyl bromide molecule, the pump–probe scheme is applied, using the same wavelengths that are used to determine the instrument time response function, but the roles of the pump and probe pulses are reversed: the molecule is excited by the pump pulse at 266 nm. Subsequently, the CH_3Br molecule dissociates and the Br fragment is detected by the TOF-MS after photoionization by the delayed XUV probe pulse.

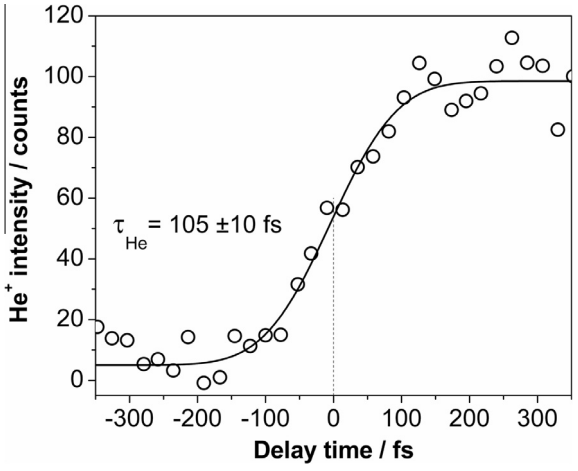

Fig. 2. Instrumental time response function determined by time-resolved spectroscopy of the instantaneous He(1s3p) absorption at an excitation energy of 54 nm (15th harmonic) and probed by time-delayed ionization with a 266 nm pulse. The open symbols represent the measured data while the solid line is a fit to the data points assuming that the cross-correlation of the pump and probe pulses is a Gaussian function. The fit provides the t_0 time delay, as well as the width of the cross-correlation, which is found to be 105 ± 10 fs. Each data point of the transient represents the sum over the ion count yield from 10,000 pump and probe laser exposures. Five single transients were averaged to improve the signal-to-noise ratio.

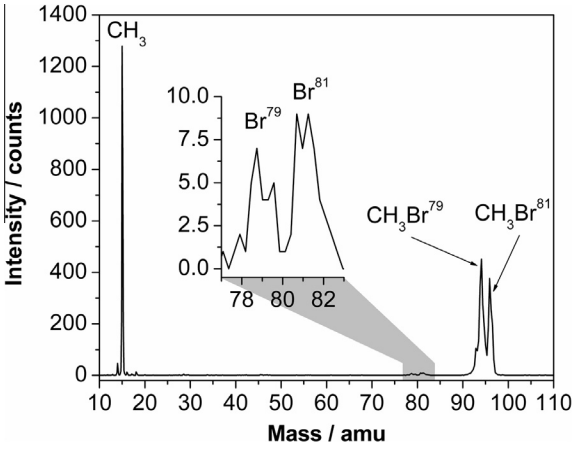

Fig. 3. Methyl bromide mass spectrum recorded at an excitation wavelength of 54 nm (15th harmonic). The spectrum has been summed over 30,000 laser pulses.

In order to distinguish between the Br^+ produced by the pump–probe transient signal and Br^+ produced by the probe beam alone (cf. Fig. 3), a chopper is installed in the pump laser beam path (cf. Fig. 1). The chopper rotates with a frequency of 500 Hz and blocks every other pump laser pulse. The integrated Br^+ peak of the mass spectrum produced by the probe pulse (XUV) alone is subtracted from the integrated Br^+ peak of the mass spectrum produced by the pump and probe pulses together. This operation, i.e. Br^+ (pump + probe) minus Br^+ (probe) is performed every two pulses, 500 times per second by the multichannel scaler/averager electronics. The resulting mass signal is summed over 30,000 laser pulses (15,000 pump + probe and 15,000 probe only) at each pump–probe time delay and is subsequently acquired by a computer. This process is repeated multiple times for different pump–probe time delays. Using this procedure of the chopper and the multichannel scaler/averager electronics, no Br^+ signal is detected by the TOF-MS when the molecules are excited by the probe beam alone (0 to 1 counts per 30,000 laser pulses [15,000 pump + probe pulses and 15,000 probe pulses only]). However, when both pump and probe beams are employed at a positive time delay larger than 200 fs, an average Br^+ signal of about 10 counts is detected per 30,000 laser pulses. This Br^+ transient subtraction technique could not be applied with the same accuracy to monitor the transient changes of the parent molecule or the CH_3 fragment, because of the high probe-only signal intensity.

Fig. 4 shows the temporal evolution of the Br^+ signal intensity as a function of the pump–probe delay time. In this plot, the average pump intensity (about 3×10^8 W/cm^2) has been carefully adjusted so that no ion signals are produced by the pump pulse alone. To improve the signal-to-noise ratio, 60 single transients are also averaged (60 × [15,000 + 15,000] laser pulses). The open symbols in Fig. 4 represent the experimental data. The Br^+ transient signal displays an abrupt rise that starts close to the zero pump–probe time delay and it reaches a maximum around 200 fs. Subsequently, the transient signal intensity does not change, which is a key point in the proof that the signal arises from the ionization of free Br atoms and not from the parent electronically excited molecule, discussed further below.

In general the molecular repulsive potentials, e.g. the CH_3Br A-band curves, can lead to product formation with a time behavior that can be described as a single exponential decay function [24,25]. Consequently, in experiments that can monitor the change of the molecular electronic structure during the dissociation, i.e.

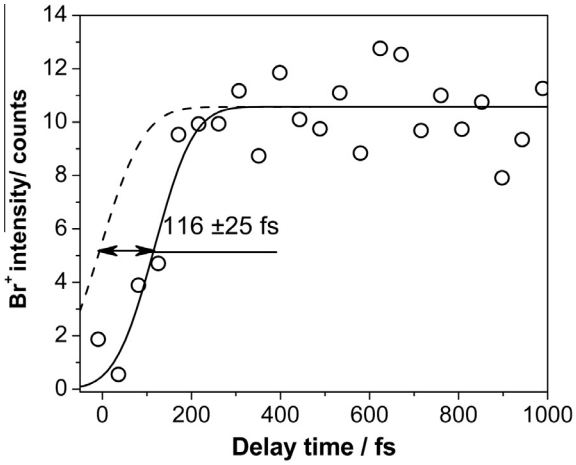

Fig. 4. Transient obtained by monitoring the Br^+ signal as a function of the pump–probe time delay (open symbols). The solid line represents the best fit of a fast rise function model [step function convoluted with the autocorrelation function, the same model as in Fig. 2(b)] to the measured data. The central wavelengths of the pump and probe pulses are 266 nm and 54 nm, respectively. The dashed curve represents the fit of the instrumental time response function from Fig. 2(b) flipped horizontally around the zero time delay and normalized to the Br^+ transient signal.

photoelectron spectroscopy or transient absorption spectroscopy, the transient signals corresponding to the formation of the fragments can be fitted by a single exponential function convoluted with the pump–probe autocorrelation function [26]. However, when the ultrafast molecular dissociation dynamics is investigated by detecting fragment ions by mass spectrometry and the measured transient signal occurs on a comparable time scale as the instrumental time response function, the transient fragment signals turn on abruptly when the intramolecular distance is large enough and the fragments are fully formed. In this case, the transient signals can be fitted by a step function convoluted with the pump–probe autocorrelation function [27].

The solid line in Fig. 4 represents the best fit to the measured data by a delayed fast rise function, which is a step function convoluted with the pump–probe autocorrelation function. The fast rise of the Br^+ transient signal is characteristic of direct gas-phase dissociation. The Br^+ transient signal is measured to be delayed by 116 ± 25 fs with respect to the He transient signal (cf. dashed curve in Fig. 4).

4. Discussion

4.1. Pump pulse excitation

Power dependence measurements performed on the CH_3Br molecule irradiated by the pump beam alone, at 266 nm, show that the molecule can be dissociatively ionized by means of three photons. As noted, in the experiment the pump power has been carefully reduced, such that ions from neither the parent molecule nor the fragments are detected by the TOF-MS with the pump beam alone. Therefore, the origin of the Br^+ transient signal in Fig. 4 is not due to dissociative ionization of the parent molecule by means of a three or more pump-only photon excitation, i.e. $CH_3Br \xrightarrow{266nm} CH_3Br^{*+} \longrightarrow CH_3^+ + Br$. The measured Br^+ transient signal displayed in Fig. 4 is therefore produced either by a single- or two-photon pump excitation followed by the probe pulse ionization.

Due to the very low intensity of the Br^+ transient signal, pump power dependence measurements could not be made. Therefore in the next section the various excitation scenarios gleaned from previous spectroscopic investigations and results here are considered, providing insight into the likely pathways and the origin of the Br^+ signal.

Fig. 5 illustrates the energy diagram of CH_3Br adapted from Escure et al [11,28] as well as the possible excitation mechanisms at 266 nm. Previous non-time-resolved gas-phase photodissociation investigations of CH_3Br demonstrate that the photodissociation can be induced by exciting the A-band by means of a single photon at 266 nm [10]. When the CH_3Br molecule is excited in the red wing of the A-band at this wavelength, the $^3Q_0$ and $^3Q_1$ states have significant absorption [11]. Therefore the most likely scenario is that the Br or Br*, or both, produced by the one-photon 266 nm pump is ionized by the XUV probe, and this is responsible for the Br^+ ion signal.

Another possible photodissociation channel that might be responsible for the transient Br^+ shown in Fig. 4 would be absorption of two photons of 266 nm, followed by XUV ionization. Recent photodissociation investigations of the CH_3Br molecule adsorbed at low temperature on insulating surfaces show that the molecular photodissociation can be produced by means of two photon excitation at 266 nm via the 4E state [15,16]. However, the electronic structure and the dissociation dynamics of the adsorbed CH_3Br molecule might be altered by the presence of the surface.

Theoretical investigations of the Rydberg states of the CH_3Br molecule show that the 5p Rydberg series can also be accessed at 9.3 eV (2 × 266 nm) [28]. The Rydberg states do not have a repulsive character, but a crossing between one of the Rydberg states and the 4E repulsive state is avoided and thus a potential barrier is generated through which tunneling and subsequent transition from a Rydberg to a dissociative state can occur. However, this scenario for the initial excitation of the CH_3Br, which could lead to dissociation and subsequent ionization by the XUV, is ruled out because in this case the appearance time of the Br^+ transient signal should be comparable to the lifetime of the Rydberg states, which is predicted to be about 10 ps [11].

Ion pair formation, i.e. CH_3^+–Br^-, upon excitation with two photons at 266 nm is also excluded because the threshold energy for ion pair formation in the case of CH_3Br is 9.5 eV [29,30].

As mentioned above, no pump power dependence measurements are possible due to the low intensity of the Br^+ transient signal. However, in order to find out whether a single- or a two-photon excitation process is responsible for the measured Br^+ transient signal in Fig. 4, time-dependent classical molecular dynamics simulations are performed using a similar model to the ones used by Zewail et al. [24,25] and Leone et al. [31] Two different scenarios are considered: (i) single pump photon excitation to the $^3Q_0$ state, and (ii) two photon pump excitation to the 4E state (cf. Fig. 5). The energy of the pump photon(s) represents the available energy (E_{avl})

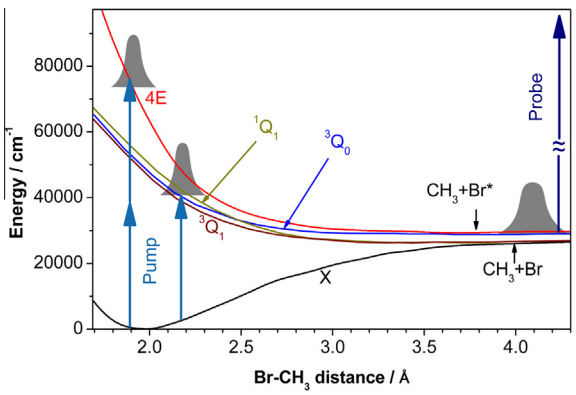

Fig. 5. Potential energy curves of the CH_3Br molecule adapted from literature [11,28]. The vertical arrows represent the excitation and the detection laser pulses. The curved arrow illustrates the propagation of the wave packet.

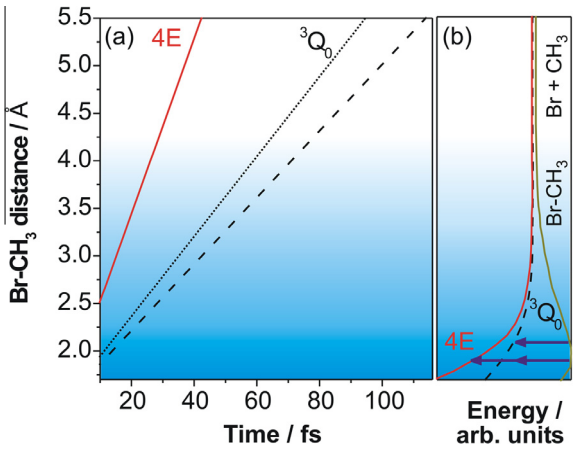

Fig. 6. (a) Classical molecular dynamics estimation of the Br–CH_3 intramolecular distance as a function of time for excitation at the central wavelength of 266 nm: (solid red curve) two-photon excitation to the 4E state when E_{AVL} is totally converted into kinetic energy; (black dotted curve) single-photon excitation of the $^3Q_0$ state when E_{AVL} is totally converted into kinetic energy; (black dashed curve) single-photon excitation of the $^3Q_0$ state when 0.4 eV of the E_{AVL} is converted into vibrational and rotational motion and the rest into kinetic energy (black solid curve). Fig. 6(b) For the sake of clarity the potential curves considered in this molecular dynamics simulation are shown together with the excitation mechanism. The blue colored area represents the non-dissociated CH_3Br molecule.

for the dissociation. During the propagation of the wave packet on the repulsive potentials, E_{avl} is converted into kinetic energy, i.e. translational energy acquired by the fragments, as well as vibrational and rotational energy. The vibrational and rotational energy released into the methyl fragment after CH_3Br photodissociation were investigated both experimentally [9,10] and theoretically [14] for various excitation wavelengths.

We consider that the repulsive potentials are of the exponential form $U(R) = U\exp(-\frac{R}{\alpha}) + U_D$, where R is the Br–CH_3 internuclear distance, U is the highest energy on the repulsive potential, $1/\alpha$ is the distance by which the energy decreases to 1/e of its initial value, and U_D is the dissociation energy. The equation of motion of the wave packet, viewed as a particle on the repulsive potential can be described by $\frac{\mu}{2}\left(\frac{dR}{dt}\right)^2 = E_{AVL} - U(R)$, where μ is the reduced mass of CH_3Br. The results of the numerical integration of the above equation of motion are presented in Fig. 6(a), in which the dissociation time is represented as a function of the Br–CH_3 internuclear distance for two specific repulsive states, i.e. $^3Q_0$ and 4E. For the sake of clarity the potential curves considered in this simulation are shown in Fig. 6(b). In the case of single-photon dissociation via the $^3Q_0$ state, two different situations are considered: (i) E_{AVL} is totally converted into kinetic energy (black dotted curve in Fig. 6(a)), and (ii) 0.4 eV of the E_{AVL} is converted into internal vibrational and rotational motion and the rest into kinetic energy (black dashed curve in Fig. 6(a)) [14]. If we consider that the dissociation has occurred in the region where the potential energy reaches a plateau on the repulsive potentials, which corresponds to a Br–CH_3 internuclear distance of about 4.25 Å [11] (cf Fig. 6(b)), and the E_{AVL} is converted all into kinetic energy (no energy goes into vibrational or rotational motion), the dissociation time is 29 fs on the 4E state and 65 fs for the $^3Q_0$ state. If 0.4 eV from E_{AVL} is converted into vibrational and rotational motion, the dissociation on the $^3Q_0$ state occurs in 79 fs. Unfortunately, the amount of energy converted into vibrational and rotational motion for the dissociation on the 4E state is unknown. In order to match to the experimental results, the amount of internal energy associated with the dissociation via 4E state should be considerably larger than the kinetic energy of the fragments, which is very unlikely, therefore this dissociation channel is ruled out.

Considering that the dissociation occurs on the $^3Q_0$ state (cf Fig. 6(a)), a Br–CH_3 internuclear distance of 5.5 Å corresponds to the dissociation time measured in our experiment, i.e. 116 fs. Although the present simulation is not accurate enough to perfectly reproduce the experimental results, it supports the hypothesis that the CH_3Br molecule is dissociated by a single pump photon.

4.2. Probe pulse ionization

In this section, we consider other possible pathways associated with the XUV probe that could lead to the measured Br^+ transient signal in Fig. 4. The probe pulse, i.e. 15th harmonic of the fundamental wavelength has enough energy to excite the CH_3Br molecule from the ground state into an excited cationic state that could lead to fragmentation (dissociative ionization) and produce the Br^+ signal as observed in Fig. 3. It is clear that this Br^+ background signal produced by the probe beam alone is reduced to zero by using the chopper as explained in the 'Results' section and has no influence on the Br^+ transient signal.

Another pertinent pathway is whether or not the probe pulse can ionize the initially excited molecule, termed CH_3Br^* here, in the A-band, and if this would have an influence on the observed Br^+ transient signal. The dissociative ionization from the A-band should result in a Br^+ transient signal immediately after excitation, close to the zero pump–probe time delay. In previous gas-phase experiments the dissociative ionization of CH_3I excited into the A-band is reflected by a transient peak structure with a maximum near zero pump–probe time delay [27,32]. To consider this possibility, in Fig. 7 a transient signal is simulated by convoluting the cross correlation curve of the pump and probe laser pulses with a single exponential decay function. In this simulation we assume that the A-band of the CH_3Br molecule decays exponentially with a time constant of 116 fs that corresponds to the observed delay of the transient Br^+ ion signal in the present experiment (cf. Fig. 4). The simulated transient signal in Fig. 7 has a peak shape (filled curve). It reaches its maximum intensity at a pump–probe time delay of 65 fs, which is the highest overlap area between the Gaussian and the single exponential decay functions. If the Br^+ transient signal would be produced by dissociative ionization of the CH_3Br^* molecule by the probe pulse directly from A-band, before the

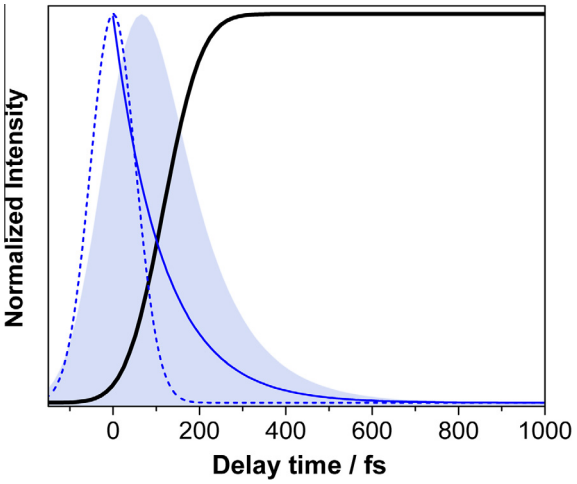

Fig. 7. Simulation of the transient signal that would be detected if the CH_3Br molecule is ionized directly from the excited A-band with the XUV probe pulse (filled curve). The simulated transient signal is a convolution of a cross correlation curve of the pump and probe laser pulses (dashed line) with a single exponential decay function with a time constant of 116 fs (solid line). The thick solid line represents the fit to the measured Br^+ signal from Fig. 4.

A-band decay, a transient peak structure similar to the one displayed in Fig. 7 should be detected in the experiment. However, in the experiment the Br^+ transient rises and stays constant, rather than diminishing again. Therefore, the best interpretation is that the Br^+ rises with the decay of the A-band (cf. Fig. 7 solid curve), which is correlated with the loss of CH_3Br^*. Moreover, dissociative ionization of a molecule like CH_3Br typically results in $CH_3^+ + Br$, rather than $CH_3 + Br^+$, and arguments can be given that this may also hold for CH_3Br^*. This is due to the higher electronegativity of Br (2.96) with respect to CH_3 (2.40). Therefore, after dissociative photoionization of CH_3Br by XUV radiation the Br atom attracts the electrons toward itself and will remain as a neutral fragment while the CH_3 radical appears in the mass spectrum as a cation. This suggests the explanation for the extremely low intensity of the Br fragment signal in Fig. 3. Consequently, even if the probe beam does dissociatively ionize the CH_3Br molecule from the excited A-band, most of the resulting bromine atoms would be neutral and not influence the observed transient signal in Fig. 4.

4.3. Pump–probe dissociation dynamics

As mentioned in the 'Introduction', the direct dissociation time of the free CH_3Br molecule via A-band excitation has not been probed before. However, Gougousi et al., using the anisotropy parameter β deduced from velocity map imaging experiments at wavelengths between 215 nm and 250 nm, estimated a CH_3Br dissociation time of 120 ± 40 fs for the formation of Br^* [9]. Using the same method, but focused on the red wing absorption of the A-band, Underwood and Powis obtained a value 111 fs for the formation of Br^* which occurs entirely on the $^3Q_0$ state and 188 fs for the formation of Br [10].

As mentioned earlier, when the CH_3Br molecule is excited in the red wing of the A-band, the $^3Q_0$ and $^3Q_1$ states have significant absorption [10,11]. Consequently, two dissociation channels might contribute to the Br^+ transient signal displayed in Fig. 4 and the coherent delay measured in Fig. 4 most likely corresponds to the faster dissociation channel, which according to literature estimates is the $^3Q_0$ state.

The classical molecular dynamics simulations (see subsection A) indicate that the CH_3Br dissociation occurs due to a single photon excitation to the A-band. Moreover, the CH_3Br dissociation time measured in the present experiment is in good agreement with the estimated dissociation time available in literature for the $^3Q_0$ state excitation that correlates with the formation of the Br^* channel [9,10]. Therefore, it is likely that the Br^+ transient signal displayed in Fig. 4 is primarily due to single pump photon dissociation via $^3Q_0$. Furthermore, the extremely low intensity of the Br^+ transient signal in Fig. 4 can be explained by the low absorption cross section of CH_3Br when excited by a single photon at the central wavelength of 266 nm, i.e. 5.1×10^{22} cm^2 $molec^{-1}$ [4,33–35].

The photodissociation dynamics in our experiment can be concluded as follows. Immediately after photoexcitation, before the fragments are separated, the probe pulse can directly ionize the excited molecule from the A-band and produce dissociative photoionization that results in the formation of neutral Br and positively charged CH_3, due to the high electronegativity value of Br fragment (see the discussion in the sub section B). After photoexcitation, once the fragments are far enough apart and the electronegativity difference of the fragments does not play an important role, a positively charged Br fragment can be produced by the probe pulse and detected. Consequently, the coherent time delay of 116 ± 25 fs of the Br^+ transient signal in Fig. 4 represents the time required for the Br fragments to completely separate from the CH_3, so that the electronic structures of the fragments are not influenced by each other.

5. Conclusion

In this paper the ultrafast photodissociation dynamics of CH_3Br in the red wing of the A-band has been investigated in a pump–probe experiment as well as by classical molecular dynamics. The CH_3Br molecule was dissociated by the pump laser pulse at the central wavelength of 266 nm. Evidence indicates that the observed fragmentation channel in this investigation is due to the excitation of the $^3Q_0$ state of the A-band, which leads to the formation of Br^* and CH_3. The probe laser pulse in the XUV spectral domain ionizes the Br fragment just after the complete separation from CH_3 radical. No indications of dissociative ionization have been found to contribute to the detected Br^+ transient signal, presumably because the electronegativity value of Br is higher than the electronegativity value of CH_3, which makes the electrons more attracted to the Br fragment than to the CH_3. After dissociative ionization the CH_3 fragments are positively charged and most of the Br fragments are neutral and are not contributing to the observed transient signal. The CH_3Br dissociation time of 116 ± 25 fs measured in the present investigation is in a very good agreement with the dissociation time calculated using the anisotropy parameter β [9,10].

Acknowledgements

The authors gratefully acknowledge financial support provided by the U.S. Air Force Office of Scientific Research (Grant No. FA9550-13-1-0094)

References

[1] L.T. Molina, M.J. Molina, F.S. Rowland, J. Phys. Chem. 86 (1982) 2672.
[2] W.S. Felps, K. Rupnik, S.P. McGlynn, J. Phys. Chem. 95 (1991) 639.
[3] W.B. DeMore, S.P. Sander, D.M. Golden, R.F. Hampson, M.J. Kurylo, C.J. Howard, A.R. Ravishankara, C.E. Kolb, M.J. Molina, Chemical kinetics and photochemical data for use in stratospheric modeling, Evaluation No. 11. JPL Publication 94–26, Jet Propulsion Laboratory: Pasadena, CA, (1994).
[4] S.P. Sander, R.R. Friedl, A.R. Ravishankara, D.M. Golden, C.E. Kolb, M.J. Kurylo, M.J. Molina, G.K. Moortgat, H. Keller-Rudek, J.B. Finlayson-Pitts, P.H. Wine, R.E. Huie, V.L. Orkin, Chemical Kinetics and Photochemical Data for Use in Atmospheric Studies, Evaluation No. 15. JPL Publication 06–2, Jet Propulsion Laboratory: Pasadena, CA, (2006).
[5] G.N.A. Van Veen, T. Baller, A.E. De Vries, Chem. Phys. 92 (1985) 59.
[6] W.P. Hess, D.W. Chandler, J.W. Thoman Jr, Chem. Phys. 163 (1992) 277.
[7] V. Blanchet, P.C. Samartzis, A.M. Wodtke, J. Chem. Phys. 130 (2009) 034304.
[8] M.L. Lipciuc, M.H.M. Janssen, J. Chem. Phys. 127 (2007) 224310.
[9] T. Gougousi, P.C. Samartzis, T.N. Kitsopoulos, J. Chem. Phys. 108 (1998) 5742.
[10] J.G. Underwood, I. Powis, Phys. Chem. Chem. Phys. 1 (2000) 747.
[11] C. Escure, T. Leininger, B. Lepetit, J. Chem. Phys. 130 (2009) 244305.
[12] R. de Nalda, J. Dura, A. Garcia-Vela, J.G. Izquierdo, J. Gonzalez-Vazquez, L. Banares, J. Chem. Phys. 128 (2008) 244309.
[13] R. de Nalda, J.G. Izquierdo, J. Dura, L. Banares, J. Chem. Phys. 126 (2007) 021101.
[14] C. Escure, T. Leininger, B. Lepetit, Chem. Phys. Lett. 480 (2009) 62.
[15] M.E. Vaida, T. Gleitsmann, R. Tchitnga, T.M. Bernhardt, Phys. Status Solidi B 247 (2010) 1139.
[16] M.E. Vaida, T.M. Bernhardt, Faraday Discuss. 157 (2012) 437.
[17] M.E. Vaida, T.M. Bernhardt, C. Barth, F. Esch, U. Heiz, U. Landman, Phys. Status Solidi B 247 (2010) 1001.
[18] M.E. Vaida, T.M. Bernhardt, Chem. Phys. Chem. 11 (2010) 804.
[19] C.G. Wahlstrom, J. Larsson, A. Persson, T. Starczewski, S. Svanberg, P. Salieres, P. Balcou, A. L'Huillier, Phys. Rev. A 48 (1993) 4709.
[20] P. Balcou, A. L'Huillier, D. Escande, Phys. Rev. A 53 (1996) 3456.
[21] J. Zhou, J. Peatross, M.M. Murnane, H.C. Kapteyn, I.P. Christov, Phys. Rev. Lett. 76 (1996) 752.
[22] K.J. Schafer, K.C. Kulander, Phys. Rev. Lett. 78 (1997) 638.
[23] A. Johansson, M.K. Raarup, Z.S. Li, V. Lokhnygin, D. Descamps, C. Lyngå, E. Mevel, J. Larsson, C.G. Wahlström, S. Aloise, M. Gisselbrect, M. Meyer, A. L'Huillier, Eur. Phys. J. D 22 (2003) 3.
[24] R. Berson, A.H. Zewail, Ber. Bunsen-Ges. Phys. Chem. 92 (1988) 373.
[25] G. Roberts, A.H. Zewail, J. Phys. Chem. 95 (1991) 7973.
[26] P. Wernet, Phys. Chem. Chem. Phys. 13 (2011) 16941.
[27] D. Zhong, A.H. Zewail, J. Phys. Chem. A 102 (1998) 4031.
[28] C. Escure, T. Leininger, B. Lepetit, J. Chem. Phys. 130 (2009) 244306.
[29] K. Suto, Y. Sato, C.L. Reed, V. Skorokhodov, Y. Matsumi, M. Kawasaki, J. Phys. Chem. A 101 (1997) 1222.

[30] T. Munakata, T. Kasuya, Chem. Phys. Lett. 154 (1989) 604.
[31] L. Nugent-Glandorf, M. Scheer, D.A. Samuels, V.M. Bierbaum, S.R. Leone, J. Chem. Phys. 117 (2002) 6108.
[32] D. Zhong, P.Y. Cheng, A.H. Zewail, J. Chem. Phys. 105 (1996) 7864.
[33] L.T. Molina, M.J. Molina, F.S. Rowland, J. Phys. Chem. 86 (1982) 2672.
[34] A.P. Uthman, P.J. Demlein, T.D. Allston, M.C. Withiam, M.J. McClements, G.A. Takacs, J. Phys. Chem. 82 (1978) 2252.
[35] N. Davidson, J. Am. Chem. Soc. 73 (1951) 467.